JOC The Journal of Organic Chemistry

Article

Cite This: J. Org. Chem. 2019, 84, 13565−13571

pubs.acs.org/joc

Theoretical Study of Diastereoselective NHC-Catalyzed Cross-Benzoin Reactions between Furfural and *N*-Boc-Protected α-Amino Aldehydes

Abing Duan,[†,⊥] Jason S. Fell,[‡,⊥] Peiyuan Yu,[‡] Colin Yu-hong Lam,[‡] Michel Gravel,[*,§] and K. N. Houk[*,‡]

[†]College of Environmental Science and Engineering, Hunan University, Changsha, Hunan 410082, China

[‡]Department of Chemistry and Biochemistry, University of California Los Angeles, Los Angeles, California 90095-1569, United States

[§]Department of Chemistry, University of Saskatchewan, 110 Science Place, Saskatoon, Saskatchewan S7N 5C9, Canada

Supporting Information

ABSTRACT: The mechanism and origins of *syn* and *anti* selectivity of cross-benzoin reactions between furfural and α-amino aldehydes, catalyzed by a triazolium-based NHC, were investigated using density functional theory calculations. *N*-Boc-α-amino aldehydes were found to react with *anti* selectivity, while *N*-Bn-*N*-Boc-α-amino aldehydes react with *syn* selectivity. We find that the *anti* product is more thermodynamically favored than the *syn* product for reactions with *N*-Boc-α-amino aldehydes, and that the formation of the *syn* product for reactions involving *N*-Bn-*N*-Boc-α-amino aldehydes is kinetically favored. The switch in selectivity is a result of an intramolecular hydrogen bond in the *N*-Boc-α-amino aldehyde, whereas switching to *N*-Bn-*N*-Boc-α-amine removes the hydrogen bond. The steric and electronic interactions in the transition state are rationalized by a Felkin−Anh model.

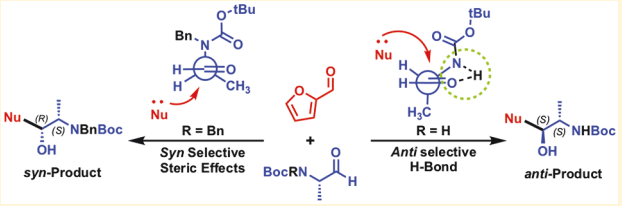

INTRODUCTION

The benzoin reaction, first reported in 1832 by Wöhler and Liebig,[1] produces an acyloin from the coupling of two aldehydes. Ukai et al.[2] and Breslow[3] later reported the use of the *N*,*S* carbene from thiazolium salts as catalysts for the benzoin reaction. The use of *N*-heterocyclic carbenes (NHC) to catalyze benzoin reactions has been widely reported in recent years.[4] The homocoupling of aldehydes in high enantioselectivity is now possible with a variety of chiral NHCs.[5] However, the coupling between two different aldehydes in cross-benzoin reactions is substantially more challenging because four products can form: two homobenzoin (Scheme 1a,b) and two cross-benzoin products (Scheme 1c,d).[6]

Recently, the Gravel group developed a chemoselective cross-benzoin reaction between aromatic and aliphatic aldehydes catalyzed by triazolium-based NHCs.[7] Experimental and computational studies explored the kinetics and the formation of an NHC adduct (Breslow intermediate)[3] with aliphatic aldehydes.[8] Previous studies performed by Connon and co-workers have demonstrated that the electronic nature and steric bulk of the substrates greatly affect the chemoselectivity in cross-benzoin reactions.[9] The Gravel group further demonstrated that installing bulky electron-withdrawing groups close to the reaction center can further influence chemoselectivity. *N*-Boc-protected α-amino aldehydes were found to be excellent partners with either aliphatic or hetereoaromatic aldehydes, and the reactions are diastereoselective (Scheme 2, entries 1−3).[10] *N*-Bn-*N*-Boc-α-amino aldehydes (Scheme 2, entry 4) still afford high chemo-

Scheme 1. General Cross-Benzoin Reaction

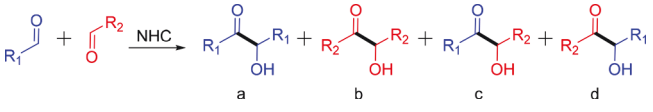

Scheme 2. Chemoselective and Diastereoselective NHC-Catalyzed Cross-Benzoin Reactions

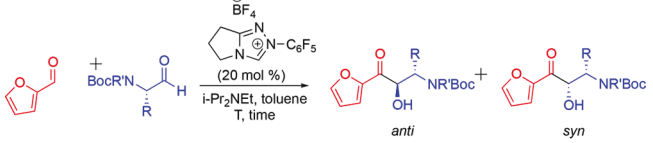

R	R'	T (°C)	time (h)	Yield (%)	*anti* : *syn*
Me	H	70	4	73	2 : 1
iPr	H	70	4	73	7 : 1
Bn	H	70	4	73	3 : 1
Me	Bn	40	1	69	1 : 5

Received: July 5, 2019
Published: September 12, 2019

DOI: 10.1021/acs.joc.9b01821
J. Org. Chem. 2019, 84, 13565−13571

selectivity, but the diastereoselectivity reverses.[11] Specifically, *N*-Boc-protected α-amino aldehydes mainly afford the *anti* products, while the *N*-Bn-*N*-Boc-α-amino aldehyde leads to *syn* products (Scheme 2, entry 4).

The reversal in diastereoselectivities for these α-amino aldehydes was rationalized by the presence of a hydrogen bond occurring between the *N*-Boc and aldehyde groups (Scheme 3a).[11] This hydrogen bond induces the groups on the α-carbon

Scheme 3. Cross-Benzoin Reactions[a]

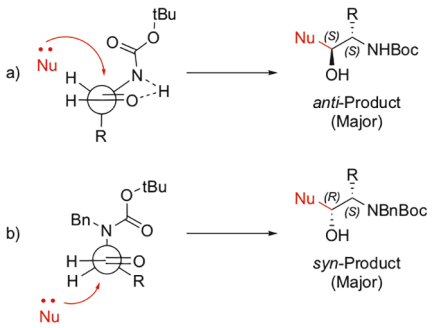

[a](a) The cross-benzoin reaction of *N*-Boc-α-amino aldehydes yields the *anti* product as the major product. (b) The cross-benzoin reaction with *N*-Bn-*N*-Boc-α-amino aldehydes gives the *syn* product.

to be in a conformation that places the R group *anti* to the approaching nucleophile. When the *N*-H is replaced with *N*-Bn, this hydrogen bond is lost, and the α-carbon rotates into a different conformation that places the R group *syn* to the approaching nucleophile (Scheme 3b).

The proposed mechanism for the NHC-catalyzed cross-benzoin reaction of 2-furaldehyde and protected α-amino aldehyde is shown in Scheme 4.[3,12] Deprotonation of the

Scheme 4. Proposed Mechanism of NHC-Catalyzed Cross-Benzoin Reaction

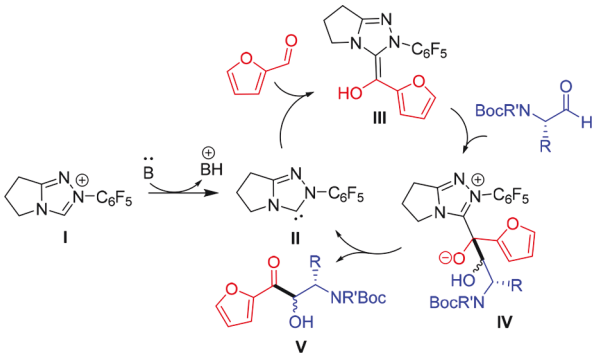

triazolium precatalyst (**I**) generates the active NHC catalyst (**II**). This nucleophilic species preferentially attacks furfural to form the Breslow intermediate (**III**). The Breslow intermediate then attacks the α-amino aldehyde and undergoes a proton transfer (**IV**). Collapse of this intermediate (**IV**) releases the cross-benzoin product (**V**) and regenerates the catalyst to repeat the cycle.[7,8]

Density functional theory (DFT) investigations into the benzoin reaction have been reported.[8,13] Although some of these studies have explored the origins of enantioselectivity using chiral catalysts,[13a,e,f] none has focused on the use of chiral substrates. This latter scenario introduces the additional challenge of determining whether the kinetic or thermodynamic control is responsible for the observed diastereoselectivities. Rehbein et al. investigated both experimentally and computationally whether the Breslow intermediate in the benzoin condensation could form a radical pair via a single-electron process and concluded that the nonradical pathway is more significant.[13h] We have now performed a DFT study to investigate the detailed mechanism of cross-benzoin reactions involving chiral α-amino aldehydes. Our computational results provide a rationale for the reported diastereoselectivities and underscore the fine interplay between kinetic and thermodynamic controls.

COMPUTATIONAL METHODS

All DFT calculations were performed using the Gaussian 09 software package.[14] Gas-phase ground state and transition state geometries were optimized with the B3LYP functional[15] and the 6-31G(d) basis set. Geometry optimizations were followed by single-point calculations using the B3LYP function with Grimme's dispersion correction[16] (B3LYP-D3(BJ)) and the def2-TZVPP[17] basis set in toluene using the SMD[18] solvent model. These methods have been shown to give good results in related stereoselectivity studies.[19] Vibrational frequencies were computed at the B3LYP/6-31G(d) level to determine if the optimized structures are minima or saddle points on the potential energy surface corresponding to ground state and transition state geometries, respectively. Free energies were calculated for 1 atm at 298.15 K. Conformational searches were performed using the MMFF force field in Maestro 11.0.[20] We utilized the Monte Carlo multiple minimum method with Oren−Speidcato variable metric minimization for optimized conformational sampling.[21] Molecular structures are displayed with CYLview.[22]

RESULTS AND DISCUSSION

Gravel et al. previously reported DFT studies of the homo- and cross-benzoin reactions of alkyl and aryl aldehydes.[8] The active carbene catalyst (**II**) reacts with furfural to generate the Breslow intermediate (**III**). The lowest energy configuration of the Breslow intermediate, (***E*)-*s*-*trans***, undergoes subsequent reactions. In this conformation, the oxygen of the furyl moiety is oriented toward the electron-poor pentafluorophenyl substituent. A full analysis of the major Breslow intermediate configurations is provided in the Supporting Information (Figure S1).

We first investigated the mechanism of the cross-benzoin reaction between (***E*)-*s*-*trans*** and ***N*-Boc-alaninal**, which is illustrated in Figure 1 with free energies relative to the separated reactants. Throughout this reaction, there are four possible diastereomers for the carbon−carbon bond forming step (**TS1-a**), the subsequent intermediate (**Int-a**) and the release of the catalyst and cross-benzoin product (**TS2-a**). Each of these stereoisomers is identified by the absolute configuration of the carbons of the newly generated alcohol of the α-amino aldehyde (carbon 1, in blue) and the alcohol/alkoxide of the Breslow intermediate (carbon 2, in red). The removal of the catalyst results in the loss of a stereocenter due to the formation of a ketone, which leaves two diastereomeric products with the hydroxyl and methyl groups either *syn* or *anti* (***syn*-Prod-a** and ***anti*-Prod-a**, respectively). We have also investigated the formation of the **homo-*N*-Boc-Alininal**, **homo-furfural**, and **cross-benzoin** products and have found that these potential side products are nearly 5 to 7 kcal mol^{-1} higher in energy than that of the observed major product (***anti*-Prod-a**). This result is shown in Figure S2 in the Supporting Information.

DOI: 10.1021/acs.joc.9b01821
J. Org. Chem. 2019, 84, 13565−13571

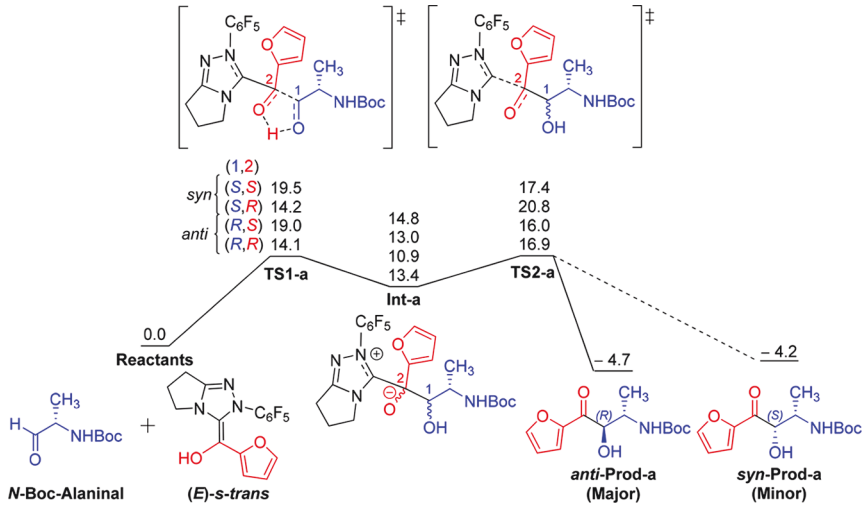

Figure 1. Free energy profile of the cross-benzoin reaction of (*E*)-***s-trans*** with ***N*-Boc-alaninal**. Each stereoisomer is identified by the absolute configuration of the two new stereocenters for carbon 1 (blue) and carbon 2 (red). The energies for each diastereomer are listed in order from top to bottom as (*S*,*S*), (*S*,*R*), (*R*,*S*), and (*R*,*R*). Energies are in units of kilocalorie per mole (kcal mol^{-1}).

The (*R*,*S*) and (*R*,*R*) diastereomers lead to the *anti* product (***anti*-Prod-a**), and the (*S*,*S*) and (*S*,*R*) diastereomers lead to the *syn* product (***syn*-Prod-a**). The formation of the cross-benzoin products is exergonic, with a preference for the *anti* product by 0.5 kcal mol^{-1}, which would give a 2:1 product ratio of *anti*:*syn*. Both nucleophilic attacks by the Breslow intermediate and loss of the NHC have similar energies leading to the unusual situation that the rate-determining steps are different for the major and minor diastereomers. The rate-determining steps for forming the *anti* and *syn* products are **TS2-a-(*R*,*R*)** and **TS1-a-(*S*,*S*)** with free energies of 16.9 and 19.5 kcal mol^{-1}, respectively. The differences in our calculated free energies for the products and rate-determining steps reveal both kinetic and thermodynamic preferences for the *anti* product (***anti*-Prod-a**), which is consistent with the experimental results shown in Scheme 2.

The nucleophilic attack of (*E*)-***s-trans*** to ***N*-Boc-alaninal** during the first step in the mechanism is the rate-determining step for producing the minor (*syn*) product. There is a 5.4 kcal mol^{-1} energy difference between the transition structures that lead to the *anti* (**TS1-a-(*R*,*R*)**) and *syn* (**TS1-a-(*S*,*S*)**) products. These transition structures are shown as Newman projections along the α-carbon-aldehyde carbon bond of ***N*-Boc-alaninal** in Figure 2. The presence of a hydrogen bond (2.12 Å) in **TS1-a-(*R*,*R*)** induces a conformation of ***N*-Boc-alaninal** that places the methyl group *anti* to (*E*)-***s-trans***, with a calculated dihedral angle of 153.7° (highlighted in green). In **TS1-a-(*S*,*S*)**, there is a weak hydrogen bond (2.97 Å), which places the methyl group gauche to the approaching (*E*)-***s-trans***, with a calculated dihedral angle of 85.8°. Thus, the stronger hydrogen bond in **TS1-a-(*R*,*R*)** induces a conformation that will place the methyl group *anti* to the incoming Breslow intermediate nucleophile in the transition state, which agrees with our proposed Felkin–Anh model.

We then investigated the cross-benzoin reaction between (*E*)-***s-trans*** and with other *N*-Boc-protected amines to observe how the size of the alkyl groups affects the diastereoselectivity. The methyl substituent was replaced with an isopropyl group (***N*-Boc-valinal**) and a benzyl group (***N*-Boc-phenylalaninal**). The relative free energy differences for the rate-determining step and of the reaction are listed in Table 1 for the reactions

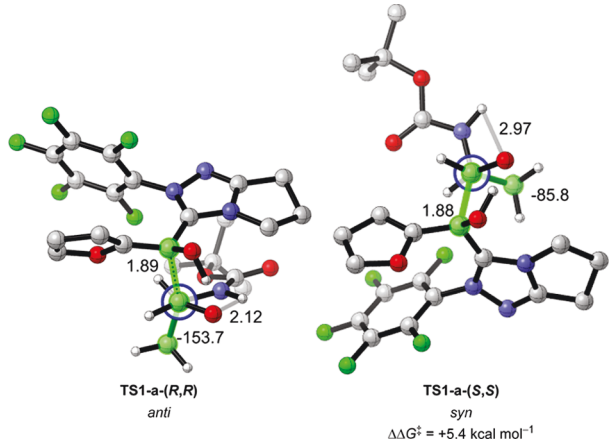

Figure 2. Newman projections of **TS1-a-(*R*,*R*)** and **TS1-a-(*S*,*S*)** for the cross-benzoin reaction of (*E*)-***s-trans*** and ***N*-Boc-alaninal** are shown with free energies. Distances for the carbon–carbon formation and hydrogen bond are in units of angstrom (Å). Atoms included in the calculated dihedral angle are highlight in green. Hydrogen atoms on the Boc group and Breslow intermediate are hidden for clarity.

with ***N*-Boc-alaninal**, ***N*-Boc-valinal**, and ***N*-Boc-phenylalaninal**. The formation of the *anti* product is thermodynamically favored in the reaction of (*E*)-***s-trans*** with ***N*-Boc-valinal** and ***N*-Boc-phenylalaninal** by 2.3 and 0.7 kcal mol^{-1}, respectively. The relative difference in energy for the rate-determining step for the reaction with ***N*-Boc-valinal** is 0.3 kcal mol^{-1}, which suggests that the barriers forming the *syn* and *anti* products are nearly isoenergetic. In all three cases, the experimentally observed *anti*:*syn* ratio more closely matches the ratio predicted by the thermodynamic control than that predicted by the kinetic control. We thus suggest that the diastereoselectivity observed in cross-benzoin reactions involving *N*-Boc amino aldehydes and 2-furaldehyde is derived from the thermodynamic control. This rationale is consistent with the observed reversibility in the formation of the cross-benzoin product[10] (see the Supporting Information for the free energy profiles of the cross-benzoin reaction of (*E*)-***s-trans*** with ***N*-Boc-valinal** (Figure S4) and ***N*-Boc-phenylalaninal** (Figure S5)).

DOI: 10.1021/acs.joc.9b01821
J. Org. Chem. 2019, 84, 13565–13571

Table 1. Differences in Free Energies of Reaction and for the Rate-Determining Steps of the Cross-Benzoin Reaction of (*E*)-*s*-*trans* with *N*-Boc-Alaninal, *N*-Boc-Valinal, and *N*-Boc-Phenylalaninal[a]

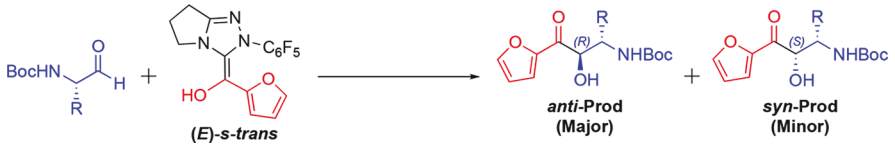

amine	R	$\Delta\Delta G^{\ddagger}$ (*anti*−*syn*)	$\Delta\Delta G_{rxn}$ (*anti*−*syn*)	predicted *anti*:*syn*	experimental *anti*:*syn*
***N*-Boc-alaninal**	ME	−2.6	−0.5	2:1	2:1
***N*-Boc-valinal**	iPr	+0.3	−2.3	33:1	7:1
***N*-Boc-phenylalaninal**	Bn	−1.8	−0.7	3:1	3:1

[a]Energies are in units of kilocalorie per mole (kcal mol^{-1}). The predicted *anti*:*syn* ratio is determined from the predicted free energy of the reaction ($\Delta\Delta G_{rxn}$).

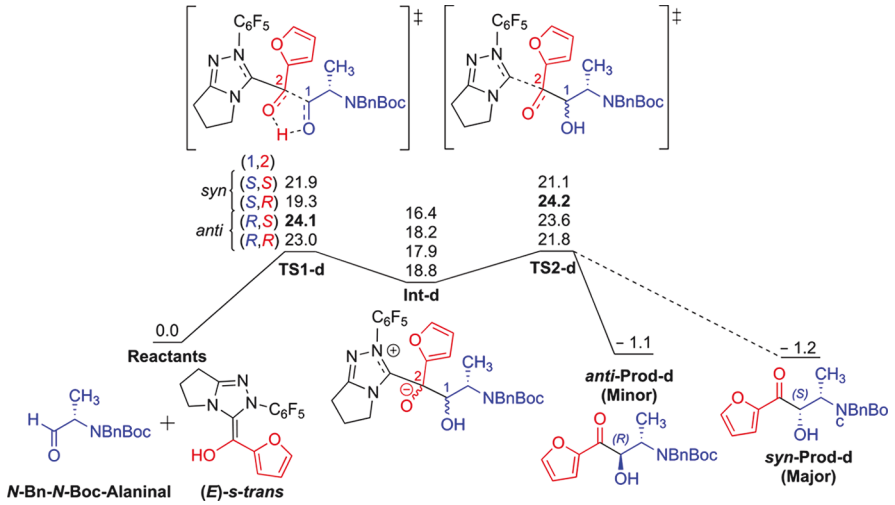

Figure 3. Free energy profile of the cross-benzoin reaction of (*E*)-***s*-*trans*** with of ***N*-Bn-*N*-Boc-alaninal**. Each stereoisomer is identified by the absolute configuration of the two new stereocenters for carbon 1 (blue) and carbon 2 (red). The energies for each diastereomer are listed in order from top to bottom as (*S*,*S*), (*S*,*R*), (*R*,*S*), and (*R*,*R*). Energies are in units of kilocalorie per mole (kcal mol^{-1}).

The *syn*/*anti* product preference for the cross-benzoin reaction of ***N*-Bn-*N*-Boc-alaninal** deviates from the previous aldehydes. The free energy profile for this reaction is illustrated in Figure 3. The major product in the cross-benzoin reaction of ***N*-Bn-*N*-Boc-alaninal** is the *syn* product, as opposed to the preference for the formation of the *anti* product for *N*-Boc-protected α-amino aldehydes. The mechanism is stepwise with the first step being the formation of a carbon−carbon bond (**TS1-d**) between (*E*)-***s*-*trans*** and ***N*-Bn-*N*-Boc-alaninal** to form the subsequent intermediate (**Int-d**). The NHC catalyst is then regenerated from the intermediate via **TS2-d**, and the products (***syn*-Prod-d** and ***anti*-Prod-d**) are released.

The free energies of formation for the *syn* and *anti* products are exergonic and are nearly isoenergetic ($\Delta\Delta G_{rxn}$ = 0.1 kcal mol^{-1}). The rate-determining steps for the formation of the *anti* and *syn* products are **TS1-d**-(*R*,*R*) and **TS1-d**-(*S*,*S*) with free energies of 23.0 and 21.9 kcal mol^{-1}, respectively. The free energies associated with **TS2-d** for these stereoisomers are within 1 kcal mol^{-1}. The predicted ratios of observed *syn*:*anti* products are 5:1 and 3:1 based upon the differences in free energies for **TS1-d** and **TS2-d**, respectively. These predicted ratios are in excellent agreement with experimental observations. These transition structures are shown as Newman projections along the α-carbon-aldehyde carbon bond of ***N*-Bn-*N*-Boc-alaninal** in Figure 4. The overall barriers computed in this case are not very different from those for the three thermodynamically-controlled reactions discussed earlier, and so the switch here to the kinetic control might seem puzzling. However, the temperature used for *N*-Bn-*N*-Boc aldehydes was somewhat lower (40 °C for 1 h) than that used for *N*-Boc aldehydes (70 °C for 4 h), and so it is conceivable that there is a switch to the kinetic control. Little selectivity is expected for the *N*-Bn-*N*-Boc case if the reaction was controlled by thermodynamics. This rationale is consistent with the erosion of the diastereomeric ratio that is observed over longer reaction times.[11]

In the previous *N*-Boc-protected systems, the alkyl substituents α to the aldehyde are placed *anti* to the nucleophile due to steric interactions and a stabilizing hydrogen bond. Without the stabilizing hydrogen bond, the sterically largest group, the *N*-Boc-*N*-Bn amino moiety, is *anti* to the nucleophile. For **TS1-d**-(*S*,*S*), the amine group on the α-carbon is nearly antiperiplanar to the approaching nucleophile (*E*)-***s*-*trans***, with a calculated dihedral angle of 152.3° (highlighted in green), and in **TS1-d**-(*R*,*R*), the calculated dihedral angle is 148.1°. In both conformations, the furfural moiety *anti* to the *N*-Boc-*N*-Bn amine, however, **TS1-d**-(*S*,*S*) experiences enhanced gauche interactions, whereas **TS1-d**-(*R*,*R*) does not. In **TS2-d**-(*S*,*S*) and **TS2-d**-(*R*,*R*), the amine group on the α-carbon remains nearly antiperiplanar to the α-carbon of the furfural moiety at 157.6° and 160.1°, respectively. **TS2-d**-(*S*,*S*) continues to experience enhanced

DOI: 10.1021/acs.joc.9b01821
J. Org. Chem. 2019, 84, 13565−13571

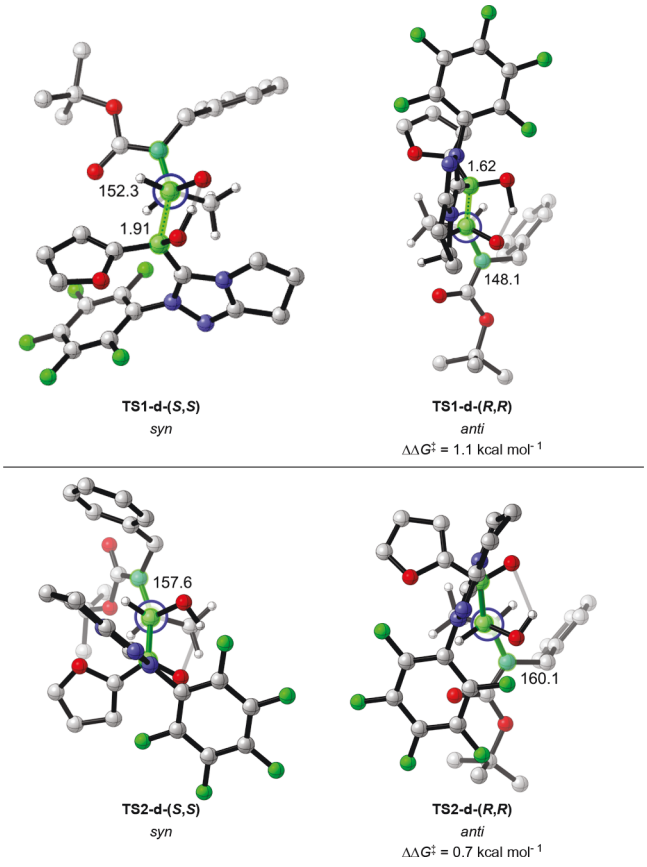

Figure 4. (top) Relative free energies (kcal mol^{-1}) and Newman projections of **TS1-d-(*S*,*S*)** and **TS1-d-(*R*,*R*)** along the C(aldehyde)−C(α) bond. (bottom) Relative free energies (kcal mol^{-1}) and Newman projections of **TS2-d-(*S*,*S*)** and **TS2-d-(*R*,*R*)** along the C(ketone)−C(α) bond. Distances are in units of angstrom (Å). Dihedral angles are highlighted in green. Hydrogens on the Boc, Bn, and NHC moieties are omitted for clarity.

gauche interactions, whereas **TS2-d-(*R*,*R*)** does not. In brief, the switch in *syn*/*anti* diastereoselectivity in the *N*-Boc-*N*-Bn series appears to be due to the lack of a hydrogen bond in these amino aldehydes and the relative placements of the sterically bulky groups based upon a Felkin−Anh model.

CONCLUSIONS

We have explored the mechanism and diastereoselectivities of the cross-benzoin reactions of α-amino aldehydes and furfural catalyzed by NHC. The cross-benzoin reaction proceeds through a stepwise mechanism. First, furfural reacts with the NHC catalyst to form a Breslow intermediate. The intermediate forms a new carbon−carbon bond with an α-amino aldehyde, which is then followed by the regeneration of the NHC. In reactions involving *N*-Boc amino aldehydes, an intramolecular hydrogen bond influences the conformation of the groups on the α-carbon, which places the alkyl group *anti* to the nucleophile. Notwithstanding this kinetic preference, our calculations support the notion that the diastereoselectivity of these reactions is under the thermodynamic control. When the amine is replaced with an *N*-Bn-*N*-Boc-protected amine, the kinetic control is necessary to obtain high diastereoselectivity. In these cases, there is a loss of the internal hydrogen bond, which induces a new conformation on the α-carbon based on the steric priorities of each group. The polar α-amino group is sterically larger than the α-alkyl substituent, which places the amine *anti* to the incoming nucleophile (Felkin−Anh selectivity). This reversal in steric priorities places the α-alkyl substituent *syn* to the newly formed hydroxyl group.

ASSOCIATED CONTENT

Supporting Information

The Supporting Information is available free of charge on the ACS Publications website at DOI: 10.1021/acs.joc.9b01821.

Geometries and energies for all chemical structures (PDF)

AUTHOR INFORMATION

Corresponding Authors

*E-mail: michel.gravel@usask.ca (M.G.).
*E-mail: houk@chem.ucla.edu (K.N.H.)

ORCID

Jason S. Fell: 0000-0001-6680-2936
Peiyuan Yu: 0000-0002-4367-6866
Colin Yu-hong Lam: 0000-0002-4946-1487
Michel Gravel: 0000-0003-3656-7108
K. N. Houk: 0000-0002-8387-5261

Author Contributions

⊥These authors contributed equally.

Notes

The authors declare no competing financial interest.

ACKNOWLEDGMENTS

We are grateful to the National Science Foundation (CHE-1361104 and CHE-1464690) and China Scholarship Council (CSC) for financial support of this research. Calculations were performed on the Hoffman2 cluster at UCLA and the Extreme Science and Engineering Discovery Environment (XSEDE), which is supported by the NSF (OCI-1053575), and the cluster at HNU, which is supported by the Fundamental Research Funds for the Central Universities. We also want to thank Dr. Wanxiang Zhao (HNU) for helpful comments.

REFERENCES

(1) Wöhler, F.; Liebig, J. Untersuchungen über das Radikal der Benzoesäure. *Ann. Pharm.* **1832**, *3*, 249.
(2) Ukai, T.; Tanaka, R.; Dokawa, T. A new catalyst for acyloin condensation. *J. Pharm. Soc. Jpn.* **1943**, *63*, 296.
(3) Breslow, R. On the Mechanism of Thiamine Action. IV.[1] Evidence from Studies on Model Systems. *J. Am. Chem. Soc.* **1958**, *80*, 3719.
(4) (a) Bugaut, X.; Glorius, F. Organocatalytic umpolung: N-heterocyclic carbenes and beyond. *Chem. Soc. Rev.* **2012**, *41*, 3511. (b) Grossmann, A.; Enders, D. N-Heterocyclic Carbene Catalyzed Domino Reactions. *Angew. Chem., Int. Ed.* **2012**, *51*, 314. (c) Flanigan, D. M.; Romanov-Michailidis, F.; White, N. A.; Rovis, T. Organocatalytic Reactions Enabled by N-Heterocyclic Carbenes. *Chem. Rev.* **2015**, *115*, 9307. (d) Izquierdo, J.; Hutson, G. E.; Cohen, D. T.; Scheidt, K. A. A continuum of progress: applications of N-hetereocyclic carbene catalysis in total synthesis. *Angew. Chem., Int. Ed.* **2012**, *51*, 11686. (e) Vora, H. U.; Wheeler, P.; Rovis, T. Exploiting Acyl and Enol Azolium Intermediates via N-Hetero- cyclic Carbene-Catalyzed Reactions of α-Reducible Aldehydes. *Adv. Synth. Catal.* **2012**, *354*, 1617. (f) Bode, J. W. An internal affair. *Nat. Chem.* **2013**, *5*, 813. (g) Ryan, S. J.; Candish, L.; Lupton, D. W. Acyl anion free N-heterocyclic carbene organocatalysis. *Chem. Soc. Rev.* **2013**, *42*, 4906. (h) Chen, X.-Y.; Ye, S. Enantioselective Cycloaddition Reactions of Ketenes Catalyzed by N-Heterocyclic Carbenes. *Synlett*

2013, *24*, 1614. (i) Hopkinson, M. N.; Richter, C.; Schedler, M.; Glorius, F. An overview of N-heterocyclic carbenes. *Nature* **2014**, *510*, 485. (j) Menon, R. S.; Biju, A. T.; Nair, V. Recent advances in employing homoenolates generated by N-heterocyclic carbene (NHC) catalysis in carbon−carbon bond-forming reactions. *Chem. Soc. Rev.* **2015**, *44*, 5040.

(5) (a) Moore, J. L.; Rovis, T. Carbene catalysts. *Top. Curr. Chem.* **2010**, *291*, 77. (b) Enders, D.; Kallfass, U. An efficient nucleophilic carbene catalyst for the asymmetric benzoin condensation. *Angew. Chem., Int. Ed.* **2002**, *41*, 1743. (c) Ma, Y.; Wei, S.; Wu, J.; Yang, F.; Liu, B.; Lan, J.; Yang, S.; You, J. From Mono-Triazolium Salt to Bis-Triazolium Salt: Improvement of the Asymmetric Intermolecular Benzoin Condensation. *Adv. Synth. Catal.* **2008**, *350*, 2645. (d) Enders, D.; Han, J. Synthesis of enantiopure triazolium salts from pyroglutamic acid and their evaluation in the benzoin condensation. *Tetrahedron: Asymmetry* **2008**, *19*, 1367. (e) Baragwanath, L.; Rose, C. A.; Zeitler, K.; Connon, S. J. Highly Enantioselective Benzoin Condensation Reactions Involving a Bifunctional Protic Pentafluorophenyl-Substituted Triazolium Precatalyst. *J. Org. Chem.* **2009**, *74*, 9214. (f) Soeta, T.; Tabatake, Y.; Inomata, K.; Ukaji, Y. Asymmetric benzoin condensation promoted by chiral triazolium precatalyst bearing a pyridine moiety. *Tetrahedron* **2012**, *68*, 894.

(6) Bugaut, X. *Comprehensive Organic Synthesis II*; Marek, I., Knochel, P., Eds.; Elsevier: Amsterdam, 2014; Vol. *1*.

(7) Langdon, S. M.; Wilde, M. M. D.; Thai, K.; Gravel, M. Chemoselective N-Heterocyclic Carbene-Catalyzed Cross-Benzoin Reactions: Importance of the Fused Ring in Triazolium Salts. *J. Am. Chem. Soc.* **2014**, *136*, 7539.

(8) Langdon, S. M.; Legault, C. Y.; Gravel, M. Origin of Chemoselectivity in N-Heterocyclic Carbene Catalyzed Cross-Benzoin Reactions: DFT and Experimental Insights. *J. Org. Chem.* **2015**, *80*, 3597.

(9) (a) Rose, C.; Gundala, S.; Connon, S. J.; Zeitler, K. Chemoselective Crossed Acyloin Condensations: Catalyst and Substrate Control. *Synthesis* **2011**, *2011*, 190. (b) O'Toole, S. E.; Rose, C. A.; Gundala, S.; Zeitler, K.; Connon, S. J. Highly Chemoselective Direct Crossed Aliphatic−Aromatic Acyloin Condensations with Triazolium-Derived Carbene Catalysts. *J. Org. Chem.* **2011**, *76*, 347.

(10) Haghshenas, P.; Gravel, M. Chemo- and Diastereoselective N-Heterocyclic Carbene-Catalyzed Cross-Benzoin Reactions Using N-Boc-α-amino Aldehydes. *Org. Lett.* **2016**, *18*, 4518.

(11) Haghshenas, P.; Quail, J. W.; Gravel, M. Substrate-Controlled Diastereoselectivity Reversal in NHC-Catalyzed Cross-Benzoin Reactions Using N-Boc-N-Bn-Protected α-Amino Aldehydes. *J. Org. Chem.* **2016**, *81*, 12075.

(12) Lapworth, A. XCVI.—Reactions involving the Addition of Hydrogen Cyanide to Carbon Compounds. *J. Chem. Soc., Trans.* **1903**, *83*, 995.

(13) (a) Dudding, T.; Houk, K. N. Computational predictions of stereochemistry in asymmetric thiazolium- and triazolium-catalyzed benzoin condensations. *Proc. Natl. Acad. Sci. U. S. A.* **2004**, *101*, 5770. (b) Yamabe, S.; Yamazaki, S. Three competitive transition states in the benzoin condensation compared to the clear rate-determining step in the Cannizzaro reaction. *Org. Biomol. Chem.* **2009**, *7*, 951. (c) He, Y.; Xue, Y. Mechanism Insight into the Cyanide-Catalyzed Benzoin Condensation: A Density Functional Theory Study. *J. Phys. Chem. A* **2010**, *114*, 9222. (d) Liu, T.; Han, S.-M.; Han, L.-L.; Wang, L.; Cui, X.-Y.; Du, C.-Y.; Bi, S. Theoretical investigation on the chemoselective N-heterocyclic carbene-catalyzed cross-benzoin reactions. *Org. Biomol. Chem.* **2015**, *13*, 3654. (e) Zhang, W.; Wang, Y.; Wei, D.; Tang, M.; Zhu, X. A DFT study on NHC-catalyzed intramolecular aldehyde-ketone crossed-benzoin reaction: mechanism, regioselectivity, stereoselectivity, and role of NHC. *Org. Biomol. Chem.* **2016**, *14*, 6577. (f) Qiao, Y.; Chen, X.; Wei, D.; Chang, J. Insights into the Competing Mechanisms and Origin of Enantioselectivity for N-Heterocyclic Carbene-Catalyzed Reaction of Aldehyde with Enamide. *Sci. Rep.* **2016**, *6*, 38200. (g) Hsieh, M.-H.; Huang, G.-T.; Yu, J.-S. K. Can the Radical Channel Contribute to the Catalytic Cycle of N-Heterocyclic Carbene in Benzoin Condensation? *J. Org. Chem.* **2018**, *83*, 15202. (h) Rehbein, J.; Ruser, S.-M.; Phan, J. NHC-catalysed benzoin condensation − is it all down to the Breslow intermediate? *Chem. Sci.* **2015**, *6*, 6013.

(14) Frisch, M. J.; Trucks, G. W.; Schlegel, H. B.; Scuseria, G. E.; Robb, M. A.; Cheeseman, J. R.; Scalmani, G.; Barone, V.; Mennucci, B.; Petersson, G. A.; Nakatsuji, H.; Caricato, M.; Li, X.; Hratchian, H. P.; Izmaylov, A. F.; Bloino, J.; Zheng, G.; Sonnenberg, J. L.; Hada, M.; Ehara, M.; Toyota, K.; Fukuda, R.; Hasegawa, J.; Ishida, M.; Nakajima, T.; Honda, Y.; Kitao, O.; Nakai, H.; Vreven, T.; Montgomery, J. A.; Peralta, J. E.; Ogliaro, F.; Bearpark, M.; Heyd, J. J.; Brothers, E.; Kudin, K. N.; Staroverov, V. N.; Kobayashi, R.; Normand, J.; Raghavachari, K.; Rendell, A.; Burant, J. C.; Iyengar, S. S.; Tomasi, J.; Cossi, M.; Rega, N.; Millam, J. M.; Klene, M.; Knox, J. E.; Cross, J. B.; Bakken, V.; Adamo, C.; Jaramillo, J.; Gomperts, R.; Stratmann, R. E.; Yazyev, O.; Austin, A. J.; Cammi, R.; Pomelli, C.; Ochterski, J. W.; Martin, R. L.; Morokuma, K.; Zakrzewski, V. G.; Voth, G. A.; Salvador, P.; Dannenberg, J. J.; Dapprich, S.; Daniels, A. D.; Farkas; Foresman, J. B.; Ortiz, J. V.; Cioslowski, J.; Fox, D. J. *Gaussian 2009*; Gaussian Inc., 2009.

(15) (a) Becke, A. D. Density-functional thermochemistry. III. The role of exact exchange. *J. Chem. Phys.* **1993**, *98*, 5648. (b) Lee, C.; Yang, W.; Parr, R. G. Development of the Colle-Salvetti correlation-energy formula into a functional of the electron density. *Phys. Rev. B: Condens. Matter* **1988**, *37*, 785.

(16) Grimme, S.; Ehrlich, S.; Goerigk, L. Effect of the damping function in dispersion corrected density functional theory. *J. Comput. Chem.* **2011**, *32*, 1456.

(17) (a) Weigend, F.; Ahlrichs, R. Balanced basis sets of split valence, triple zeta valence and quadruple zeta valence quality for H to Rn: Design and assessment of accuracy. *Phys. Chem. Chem. Phys.* **2005**, *7*, 3297. (b) Weigend, F. Accurate Coulomb-fitting basis sets for H to Rn. *Phys. Chem. Chem. Phys.* **2006**, *8*, 1057.

(18) (a) Marenich, A. V.; Cramer, C. J.; Truhlar, D. G. Universal Solvation Model Based on Solute Electron Density and on a Continuum Model of the Solvent Defined by the Bulk Dielectric Constant and Atomic Surface Tensions. *J. Phys. Chem. B* **2009**, *113*, 6378. (b) Ribeiro, R. F.; Marenich, A. V.; Cramer, C. J.; Truhlar, D. G. Use of Solution-Phase Vibrational Frequencies in Continuum Models for the Free Energy of Solvation. *J. Phys. Chem. B* **2011**, *115*, 14556.

(19) (a) Lam, Y.-h.; Grayson, M. N.; Holland, M. C.; Simon, A.; Houk, K. N. Theory and Modeling of Asymmetric Catalytic Reactions. *Acc. Chem. Res.* **2016**, *49*, 750. (b) Grayson, M. N.; Goodman, J. M. Lewis Acid Catalysis and Ligand Exchange in the Asymmetric Binaphthol-Catalyzed Propargylation of Ketones. *J. Org. Chem.* **2013**, *78*, 8796. (c) Grayson, M. N.; Goodman, J. M. Asymmetric Boronate Addition to o-Quinone Methides: Ligand Exchange, Solvent Effects, and Lewis Acid Catalysis. *J. Org. Chem.* **2015**, *80*, 2056. (d) Krenske, E. H.; Houk, K. N.; Harmata, M. Computational Analysis of the Stereochemical Outcome in the Imidazolidinone-Catalyzed Enantioselective (4 + 3)-Cycloaddition Reaction. *J. Org. Chem.* **2015**, *80*, 744. (e) Lam, Y.-h.; Houk, K. N. How Cinchona Alkaloid-Derived Primary Amines Control Asymmetric Electrophilic Fluorination of Cyclic Ketones. *J. Am. Chem. Soc.* **2014**, *136*, 9556. (f) Lam, Y.-h.; Houk, K. N. Origins of stereoselectivity in intramolecular aldol reactions catalyzed by cinchona amines. *J. Am. Chem. Soc.* **2015**, *137*, 2116. (g) Simon, A.; Lam, Y.-h.; Houk, K. N. Transition States of Vicinal Diamine-Catalyzed Aldol Reactions. *J. Am. Chem. Soc.* **2016**, *138*, 503. (h) Rodriguez, E.; Grayson, M. N.; Asensio, A.; Barrio, P.; Houk, K. N.; Fustero, S. Chiral Brønsted Acid-Catalyzed Asymmetric Allyl-(propargyl)boration Reaction of ortho-Alkynyl Benzaldehydes: Synthetic Applications and Factors Governing the Enantioselectivity. *ACS Catal.* **2016**, *6*, 2506. (i) Simon, L.; Goodman, J. M. How reliable are DFT transition structures? Comparison of GGA, hybrid-meta-GGA and meta-GGA functionals. *Org. Biomol. Chem.* **2011**, *9*, 689. (j) Moore, L. C.; Lo, A.; Fell, J. S.; Duong, M. R.; Moreno, J. A.;

DOI: 10.1021/acs.joc.9b01821
J. Org. Chem. 2019, 84, 13565−13571

Rich, B. E.; Bravo, M.; Fettinger, J. C.; Souza, L. W.; Olmstead, M. M.; Houk, K. N.; Shaw, J. T. Acyclic Stereocontrol in the Additions of Nucleophilic Alkenes to α-Chiral N-Sulfonyl−ChiralN−Sulfonyl Imines. *Chem.- Eur. J.* **2019**, *25*, 12214.
(20) *Maestro*; 11.0 ed.; Schrödinger, LLC: New York, NY, 2017.
(21) Banks, J. L.; Beard, H. S.; Cao, Y.; Cho, A. E.; Damm, W.; Farid, R.; Felts, A. K.; Halgren, T. A.; Mainz, D. T.; Maple, J. R.; Murphy, R.; Philipp, D. M.; Repasky, M. P.; Zhang, L. Y.; Berne, B. J.; Friesner, R. A.; Gallicchio, E.; Levy, R. M. Integrated Modeling Program, Applied Chemical Theory (IMPACT). *J. Comput. Chem.* **2005**, *26*, 1752.
(22) Legault, C. Y. *CYLView. 1.0b ed*; Université de Sherbrooke, 2009.

DOI: 10.1021/acs.joc.9b01821
J. Org. Chem. 2019, 84, 13565−13571